Preprints of the 21st IFAC World Congress (Virtual)
Berlin, Germany, July 12-17, 2020

Design of an integrated actuator fault-tolerant control under robust performance requirements ⋆

Mariusz Buciakowski * **Marcin Witczak** * **Marcin Pazera** *

* *Institute of Control & Computation Engineering,*
The University of Zielona Góra,
ul. Szafrana 2 65-516 Zielona Góra, Poland.
(e-mail: {M.Buciakowski, M.Witczak, M.Pazera}@issi.uz.zgora.pl).

Abstract: The paper concerns a development of an integrated design of fault estimation and control scheme within an integrated actuator fault-tolerant control framework. The integrated design boils down to avoiding a standard three-step fault diagnosis (detection, isolation, identification) and replacing it by a fault estimation. Subsequently, the inaccuracies caused by fault estimation are taken into account while designing fault-tolerant controller. Contrarily to the usual framework, which extends the set of disturbances/noise by such inaccuracies, they are taken into account individually in such a way as to achieve a well-balanced final control effect. Finally, a complete fault-tolerant design procedure is provided along with its convergence analysis. The last part of the paper shows the performance of the proposed approach using a DC-servo motor benchmark example.

Keywords: Fault-tolerant, Observer design, Robust control, Fault detection and diagnosis

1. INTRODUCTION

Fault diagnosis Blanke et al. (2006); Ding (2008); Witczak et al. (2014) and control are ones of the main pillars of modern control engineering, which aims at increasing performance of industrial systems along with their reliability. Traditionally, their integration boils down to exploiting the knowledge about the faults for restructuring the controller and maintain a possibly high system performance under faults. Note the fault is perceived as an unappealing phenomenon pertaining a deviation of at least one characteristic property of the system comparing to its nominal value. Whilst a failure stands for a complete system inability to perform a scheduled mission. The developments presented in this paper concern abnormal behaviours of actuators, which clearly mean that the fault is simply an actuator fault. Irrespective of the nature of a fault, traditional fault diagnosis can be split into three phases Blanke et al. (2006); Ding (2008); Witczak et al. (2014), i.e., detection, isolation and estimation. The first one reduces to answering the question if there is a fault while the second provides its location. Finally, the last one provides an answer concerning a possibly time-varying fault magnitude. In practice, all these three phases incorporate a degree of uncertainty into the final fault diagnosis decision, e.g., a fault detection delay, fault estimation inaccuracy, etc. Thus, efficient integration should be realized taking into account all these unappealing effects. Irrespective of these obvious facts, there are plenty of fault-tolerant-oriented works in which a perfect fault diagnosis is assumed Zhang and Jiang (2008). There is, of course, a lot of research in which full fault diagnosis is integrated within fault-tolerant control Zhang and Jiang (2008). However, managing uncertainties raised by a three-step diagnostic procedure constitutes a serious challenge both from theoretical and practical perspectives. This is the reason why an integrated and optimized fusion of Fault-Tolerant Control (FTC) and fault estimation receives a growing research attention Salazar et al. (2020); Mejdi et al. (2020); Pazera et al. (2018). Indeed, in the light of an integration, fault estimation constitutes a powerful and efficient alternative to three-step fault diagnosis. As a result, controller design aims at taking into account fault estimation inaccuracies. Thus, the usual framework is to extend the set of disturbances/noise by such inaccuracies. However, they may have different nature, size and influence onto the whole system being diagnosed and controlled. This observation raised the developments presented in this paper, which treat them individually in such a way as to achieve a well-balanced final control effect.

The paper is structured according to the following plan: Section 2 introduces the system description. Section 3 formulates the problem of an integrated design and provides structures of the fault estimator and controller, respectively. Subsequently, Sections 4 provide a convergence analysis and design procedure for a fault estimator and robust controller with section 5. Finally, Section 6 portrays the performance of the proposed approach based on a DC servo–motor benchmark example.

2. PRELIMINARY BACKGROUND

Let us start with a linear system of the form:

⋆ The work was supported by the National Science Centre of Poland under Grant: UMO-2017/27/B/ST7/00620.

$$\boldsymbol{x}_{k+1} = \boldsymbol{A}\boldsymbol{x}_k + \boldsymbol{B}\boldsymbol{u}_k + \boldsymbol{B}\boldsymbol{f}_k + \boldsymbol{W}_1\boldsymbol{w}_{1,k}, \quad (1)$$
$$\boldsymbol{y}_k = \boldsymbol{C}\boldsymbol{x}_k + \boldsymbol{W}_2\boldsymbol{w}_{2,k}, \quad (2)$$

where $\boldsymbol{x}_k \in \mathbb{R}^n$ is the state, $\boldsymbol{u}_k \in \mathbb{R}^r$ denotes the input, $\boldsymbol{y}_k \in \mathbb{R}^m$ is the output. The actuator fault is denoted by $\boldsymbol{f}_k \in \mathbb{R}^r$ while $\boldsymbol{w}_{1,k} \in \mathbb{R}^{q_1}$ and $\boldsymbol{w}_{2,k} \in \mathbb{R}^{q_2}$ stand for the system disturbance and measurements noise, respectively. Moreover, it is assumed that ith actuator fault $\boldsymbol{f}_{k,i}$ is detectable, isolable and identifiable Blanke et al. (2006). To make the paper self-contained, let us remind that

$$l_2^n = \{\mathbf{w} \in \mathbb{R}^n | \ \|\mathbf{w}\|_{l_2} < +\infty\}, \|\mathbf{w}\|_{l_2} = \left(\sum_{k=0}^{\infty} \|\boldsymbol{w}_k\|^2\right)^{\frac{1}{2}}. \quad (3)$$

Taking into account the above nomenclature, let us impose the following assumptions:

- *Assumption 1:* The process exogenous disturbance is bounded in $l_2^{q_1}$ sense, i.e., $\boldsymbol{w}_{1,k} \in l_2^{q_1}$;
- *Assumption 2:* The measurement noise is bounded in $l_2^{q_2}$ sense, i.e., $\boldsymbol{w}_{2,k} \in l_2^{q_2}$;
- *Assumption 3:* Actuator fault $\boldsymbol{f}_k$ as well as rate of fault change $\boldsymbol{\varepsilon}_k = \boldsymbol{f}_{k+1} - \boldsymbol{f}_k$ are bounded in l_2^r sense, i.e., $\boldsymbol{f}_k \in l_2^r$, $\boldsymbol{\varepsilon}_k \in l_2^r$.

Assumption 1–2 state that the exogenous disturbances $\boldsymbol{w}_{1,k}$ and $\boldsymbol{w}_{2,k}$, acting onto the system have a finite energy. Finally, *Assumption 3* signifies that any physical actuator posses a finite performance, and hence, it cannot be increased without limits. This causes that the fault rate of change cannot increase without limits as well. Indeed, in most cases it converges to zero as the fault settles at a constant level. This is the reason why most works presented in the literature Zhang and Jiang (2008) assume that $\boldsymbol{\varepsilon}_k = 0$ (or $\dot{\boldsymbol{f}} = 0$ in the continuous-time framework).

Remark 1. As stated in the title, only actuator faults are taken into account. However, the proposed strategy can be extended to handle sensor as well as system component faults. In this work, the actuator fault is treated as decrease of its performance. For example if the actuator performance decrease by 10% then a fault is estimated and the resulting estimate is employed for an appropriate fault accommodation action. This does not, of course, mean that the faults are estimated in percents. Indeed, they are expressed in the units relative to the control values. For example let us consider a dc–motor. The voltage that can be fed to this system is from 0[V] to 10[V]. If the actuator performance by 10% then the a perfect fault estimate is 1[V] and this value will be added to control signal to compensate the fault effect (Fig. 1). Finally, this 1[V] can be easily converted percent units, which can show maintenance services the current actuator performance.

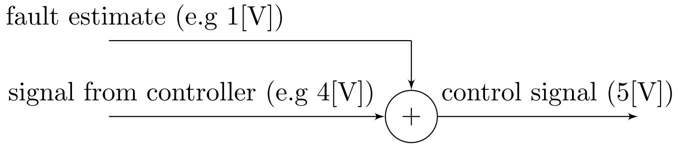

Fig. 1. System structure

Given the general description of the system, the integrated FTC will be proposed in the subsequent sections.

3. PROBLEM FORMULATION

This section undertakes two main problems (fault estimation and compensation ones) that will be investigated in this paper. Firstly, let us consider an observer of the form:

$$\hat{\boldsymbol{x}}_{k+1} = \boldsymbol{A}\hat{\boldsymbol{x}}_k + \boldsymbol{B}\boldsymbol{u}_k + \boldsymbol{B}\hat{\boldsymbol{f}}_k + \boldsymbol{K}(\boldsymbol{y}_k - \boldsymbol{C}\hat{\boldsymbol{x}}_k), \quad (4)$$
$$\hat{\boldsymbol{f}}_{k+1} = \hat{\boldsymbol{f}}_k + \boldsymbol{L}(\boldsymbol{y}_k - \boldsymbol{C}\hat{\boldsymbol{x}}_k), \quad (5)$$

where $\hat{\boldsymbol{x}}_k \in \mathbb{R}^n$ and $\hat{\boldsymbol{f}}_k \in \mathbb{R}^r$ denote the state and fault estimates. The observer design problem consists of determining the gain matrices $\boldsymbol{K} \in \mathbb{R}^{n\times m}$, and $\boldsymbol{L} \in \mathbb{R}^{r\times m}$. The structure of the proposed observer is similar to the ones presented in the literature Chen and Patton (1999); Ding (2008); Blanke et al. (2006); Isermann (2006). However, in this case it was suitably extended to estimate the magnitude of the fault. In particular, the fault estimate was included in the observer state equation (4) to improved the fault estimation quality at each step k.

Based on (1) and (2), the state estimation error $\boldsymbol{e}_k$ and fault estimation error $\boldsymbol{e}_{f,k}$ can be derived as

$$\bar{\boldsymbol{e}}_{k+1} = (\bar{\boldsymbol{A}} - \bar{\boldsymbol{K}}\bar{\boldsymbol{C}})\bar{\boldsymbol{e}}_k + (\bar{\boldsymbol{W}}_1 - \bar{\boldsymbol{K}}\bar{\boldsymbol{W}}_2)\bar{\boldsymbol{v}}_k + \boldsymbol{E}\boldsymbol{\varepsilon}_k, \quad (6)$$
$$\boldsymbol{e}_{f,k} = \bar{\boldsymbol{I}}\bar{\boldsymbol{e}}_k, \quad (7)$$

where $\bar{\boldsymbol{e}}_k = [\boldsymbol{e}_k^T, \boldsymbol{e}_{f,k}^T]^T$, $\bar{\boldsymbol{v}}_k = [\boldsymbol{w}_{1,k}^T, \boldsymbol{w}_{2,k}^T]^T$, $\boldsymbol{\varepsilon}_k = \boldsymbol{f}_{k+1} - \boldsymbol{f}_k$ and

$$\bar{\boldsymbol{A}} = \begin{bmatrix} \boldsymbol{A} & \boldsymbol{B} \\ \boldsymbol{0} & \boldsymbol{I} \end{bmatrix}, \quad \bar{\boldsymbol{K}} = \begin{bmatrix} \boldsymbol{K} \\ \boldsymbol{L} \end{bmatrix}, \quad \boldsymbol{E} = \begin{bmatrix} \boldsymbol{0} \\ \boldsymbol{I} \end{bmatrix},$$
$$\bar{\boldsymbol{W}}_1 = \begin{bmatrix} \boldsymbol{W}_1 & \boldsymbol{0} \\ \boldsymbol{0} & \boldsymbol{0} \end{bmatrix}, \quad \bar{\boldsymbol{W}}_2 = [\boldsymbol{0} \ \boldsymbol{W}_2],$$
$$\bar{\boldsymbol{I}} = [\boldsymbol{0} \ \boldsymbol{I}], \quad \bar{\boldsymbol{C}} = [\boldsymbol{C} \ \boldsymbol{0}].$$

Based on the above equation, three different objectives are considered while determining the gain matrices $\boldsymbol{K}$ and $\boldsymbol{L}$: (i) asymptotic convergence of the state and fault estimation error (6)–(7); (ii) rejection of $\bar{\boldsymbol{v}}_k$ and (iii) rejection of $\boldsymbol{\varepsilon}_k$ in the $\mathcal{H}_\infty$ sense. The above problem is formulated formally through the following definition:

Definition 1. The system (6)–(7) is robustly convergent in the $\mathcal{H}_\infty$ sense if given scalars $\mu_{o,1} > 0$ and $\mu_{o,2} > 0$:

i) (6)–(7) are asymptotically stable when $\bar{\boldsymbol{v}}_k = \boldsymbol{0}$ and $\boldsymbol{\varepsilon}_k = \boldsymbol{0}$;
ii) $\|\boldsymbol{G}_{\boldsymbol{e}_f\bar{\boldsymbol{v}}}(z)\|_\infty < \mu_{o,1}$ when $\bar{\boldsymbol{v}}_k \neq \boldsymbol{0}$;
iii) $\|\boldsymbol{G}_{\boldsymbol{e}_f\boldsymbol{\varepsilon}}(z)\|_\infty < \mu_{o,2}$ when $\boldsymbol{\varepsilon}_k \neq \boldsymbol{0}$;

where

$$\boldsymbol{G}_{\boldsymbol{e}_f\bar{\boldsymbol{v}}}(z) = \bar{\boldsymbol{I}}\left(z\boldsymbol{I} - \left(\bar{\boldsymbol{A}} - \bar{\boldsymbol{K}}\bar{\boldsymbol{C}}\right)\right)^{-1}\left(\bar{\boldsymbol{W}}_1 - \bar{\boldsymbol{K}}\bar{\boldsymbol{W}}_2\right),$$
$$\boldsymbol{G}_{\boldsymbol{e}_f\boldsymbol{\varepsilon}}(z) = \bar{\boldsymbol{I}}\left(z\boldsymbol{I} - \left(\bar{\boldsymbol{A}} - \bar{\boldsymbol{K}}\bar{\boldsymbol{C}}\right)\right)^{-1}\boldsymbol{E},$$

denote the transfer functions from the input $\bar{\boldsymbol{v}}_k$ and $\boldsymbol{\varepsilon}_k$ to the output $\boldsymbol{e}_{f,k}$ respectively.

Note that the usual approach is to treat ε_k and $\boldsymbol{e}_{f,k}$ as a coupled disturbance vector. However, as observed by the authors, this may lead to an increased conservativeness as they may operate on completely different magnitude levels.

The second problem to be addressed is to design fault compensation scheme for (1)–(2) , which is proposed as:

$$\boldsymbol{u}_k = -\boldsymbol{F}\boldsymbol{x}_k - \hat{\boldsymbol{f}}_k. \quad (8)$$

By defining $\boldsymbol{v}_k = [\boldsymbol{w}_{1,k}^T, \boldsymbol{w}_{2,k}^T]^T$ and applying the control strategy to (1)–(2), one can show that:

$$\boldsymbol{x}_{c,k+1} = (\boldsymbol{A} - \boldsymbol{B}\boldsymbol{F})\boldsymbol{x}_{c,k} + \boldsymbol{B}\boldsymbol{e}_{f,k} + [\boldsymbol{W}_1 \ \boldsymbol{0}]\,\boldsymbol{v}_k, \quad (9)$$

$$\boldsymbol{y}_k = \boldsymbol{C}\boldsymbol{x}_{c,k} + [\boldsymbol{0} \ \boldsymbol{W}_2]\,\boldsymbol{v}_k. \quad (10)$$

where $\boldsymbol{x}_{c,k} \in \mathbb{R}^n$ represent the state of close loop system. Based on the above equations, three different objectives are considered while determining the gain matrix $\boldsymbol{F}$ for the control strategy (8): (i) asymptotic convergence to zero of the state $\boldsymbol{x}_{c,k}$ and (ii)–(iii) rejection of $\boldsymbol{v}_k$ and $\boldsymbol{e}_k$ in the $\mathcal{H}_\infty$ sense. The above problem is formally formulated through the following definition:

Definition 2. The close loop system (9)–(10) is robustly convergent in the $\mathcal{H}_\infty$ sense if given scalars $\mu_{c,1} > 0$ and $\mu_{c,2} > 0$:

i) (9)–(10) are asymptotically stable when $\boldsymbol{v}_k = \boldsymbol{0}$ and $\boldsymbol{e}_{f,k} = \boldsymbol{0}$
ii) $\|\boldsymbol{G}_{\boldsymbol{y}\boldsymbol{v}}(z)\|_\infty < \mu_{c,1}$ when $\boldsymbol{v}_k \neq \boldsymbol{0}$
iii) $\|\boldsymbol{G}_{\boldsymbol{y}\boldsymbol{e}_f}(z)\|_\infty < \mu_{c,2}$ when $\boldsymbol{e}_{f,k} \neq \boldsymbol{0}$

where

$$\boldsymbol{G}_{\boldsymbol{y}\boldsymbol{v}}(z) = \boldsymbol{C}\left(z\boldsymbol{I} - (\boldsymbol{A} - \boldsymbol{B}\boldsymbol{F})\right)^{-1}[\boldsymbol{W}_1 \ \boldsymbol{0}] + [\boldsymbol{0} \ \boldsymbol{W}_2],$$

$$\boldsymbol{G}_{\boldsymbol{y}\boldsymbol{e}_f}(z) = \boldsymbol{C}\left(z\boldsymbol{I} - (\boldsymbol{A} - \boldsymbol{B}\boldsymbol{F})\right)^{-1}\boldsymbol{B},$$

denote the transfer functions from the input $\boldsymbol{v}_k$ and $\boldsymbol{e}_{f,k}$ to the output $\boldsymbol{y}_k$, respectively.

The controller design problem being formulated assumes that the real state $\boldsymbol{x}_k$ is available for the feedback. However, a more realistic situation is the one in which the estimated state should be used instead, i.e., (8) changes into:

$$\boldsymbol{u}_k = -\boldsymbol{F}\hat{\boldsymbol{x}}_k - \hat{\boldsymbol{f}}_k, \quad (11)$$

where $\hat{\boldsymbol{x}}_k$ is the estimated state given by the observer (4)–(5). Now, let us start by considering the system (1)–(2), the observer (4)–(5) and the control law (11). It can be shown that the overall system obeys:

$$\begin{bmatrix} \boldsymbol{x}_{c,k+1} \\ \bar{\boldsymbol{e}}_{k+1} \end{bmatrix} = \begin{bmatrix} \boldsymbol{A} - \boldsymbol{B}\boldsymbol{F} & \boldsymbol{B}\boldsymbol{F} \\ \boldsymbol{0} & \bar{\boldsymbol{A}} - \bar{\boldsymbol{K}}\bar{\boldsymbol{C}} \end{bmatrix} \begin{bmatrix} \boldsymbol{x}_{c,k} \\ \bar{\boldsymbol{e}}_k \end{bmatrix} + \begin{bmatrix} \boldsymbol{B} & \boldsymbol{0} \\ \boldsymbol{0} & \boldsymbol{E} \end{bmatrix} \begin{bmatrix} \boldsymbol{e}_{f,k} \\ \boldsymbol{\varepsilon}_k \end{bmatrix} + \begin{bmatrix} [\boldsymbol{W}_1 \ \boldsymbol{0}] \\ \bar{\boldsymbol{W}}_1 - \bar{\boldsymbol{K}}\bar{\boldsymbol{W}}_2 \end{bmatrix} \boldsymbol{v}_k, \quad (12)$$

$$\boldsymbol{y}_k = [\boldsymbol{C} \ \boldsymbol{0}] \begin{bmatrix} \boldsymbol{x}_{c,k} \\ \bar{\boldsymbol{e}}_k \end{bmatrix} + [\boldsymbol{0} \ \boldsymbol{W}_2]\,\boldsymbol{v}_k. \quad (13)$$

It can be seen that the *separation principle* holds for the asymptotic stability of (12)–(13). Indeed, the convergence of the system is defined by a union of eigenvalues of $\boldsymbol{A} - \boldsymbol{B}\boldsymbol{F}$ and $\bar{\boldsymbol{A}} - \bar{\boldsymbol{K}}\bar{\boldsymbol{C}}$. In this case, the fault/state estimator and the controller can be designed separately.

Given Definition 1 and 2, the general structure of the estimator along with its estimation error (6)–(7) and control strategy (8) along with its close loop system (12)–(13) a design procedure to determine matrices $\boldsymbol{K}$, $\boldsymbol{L}$ and $\boldsymbol{F}$ for the system (1)–(2) will be presented in the next section.

4. FAULT ESTIMATOR AND CONTROLLER DESIGN

The objective of this section is to obtain necessary and sufficient conditions for the synthesis of the observer (4)–(5) and controller (11) for the system (1)–(2), satisfying the conditions expressed by Definition 1 and 2 respectively. Using the definitions mentioned above, it is possible to formulate the two main results of this section. The first one is related to estimator design:

Theorem 1. For prescribed attenuation levels $\mu_{o,1} > 0$ and $\mu_{o,2} > 0$ of $\bar{\boldsymbol{v}}_k$ and $\boldsymbol{\varepsilon}_k$ respectively, the $\mathcal{H}_\infty$ observer design problem is solvable if and only if there exist $\boldsymbol{P} \succ \boldsymbol{0}$ and $\boldsymbol{N}$ such that the following conditions are satisfied:

$$\begin{bmatrix} \bar{\boldsymbol{I}}^T\bar{\boldsymbol{I}} - \boldsymbol{P} & * & * \\ \boldsymbol{0} & -\mu_{o,1}^2\boldsymbol{I} & * \\ \boldsymbol{P}\bar{\boldsymbol{A}} - \boldsymbol{N}\bar{\boldsymbol{C}} & \boldsymbol{P}\bar{\boldsymbol{W}}_1 - \boldsymbol{N}\bar{\boldsymbol{W}}_2 & -\boldsymbol{P} \end{bmatrix} \prec \boldsymbol{0}, \quad (14)$$

$$\begin{bmatrix} \bar{\boldsymbol{I}}^T\bar{\boldsymbol{I}} - \boldsymbol{P} & * & * \\ \boldsymbol{0} & -\mu_{o,2}^2\boldsymbol{I} & * \\ \boldsymbol{P}\bar{\boldsymbol{A}} - \boldsymbol{N}\bar{\boldsymbol{C}} & \boldsymbol{P}\boldsymbol{E} & -\boldsymbol{P} \end{bmatrix} \prec \boldsymbol{0}, \quad (15)$$

where $\boldsymbol{N} = \boldsymbol{P}\bar{\boldsymbol{K}}$. And second one is related to controller design:

Theorem 2. For a prescribed attenuation level $\mu_{c,1} > 0$ and $\mu_{c,2} > 0$ of $\boldsymbol{v}_k$ and $\boldsymbol{e}_{f,k}$, the $\mathcal{H}_\infty$ controller design problem is solvable if and only if there exist $\boldsymbol{S} \succ \boldsymbol{0}$ and $\boldsymbol{N}$ such that the following conditions are satisfied:

$$\begin{bmatrix} -\boldsymbol{S} & * & * & * \\ \boldsymbol{0} & -\boldsymbol{I} & * & * \\ \boldsymbol{S}\boldsymbol{A}^T - \boldsymbol{N}^T\boldsymbol{B}^T & \boldsymbol{S}\tilde{\boldsymbol{C}}^T & -\boldsymbol{S} & * \\ \tilde{\boldsymbol{B}}_1^T & \tilde{\boldsymbol{D}}^T & \boldsymbol{0} & -\mu_{c,1}^2\boldsymbol{I} \end{bmatrix} \prec \boldsymbol{0}, \quad (16)$$

$$\begin{bmatrix} -\boldsymbol{S} & * & * & * \\ \boldsymbol{0} & -\boldsymbol{I} & * & * \\ \boldsymbol{S}\boldsymbol{A}^T - \boldsymbol{N}^T\boldsymbol{B}^T & \boldsymbol{S}\tilde{\boldsymbol{C}}^T & -\boldsymbol{S} & * \\ \tilde{\boldsymbol{B}}_2^T & \boldsymbol{0} & \boldsymbol{0} & -\mu_{c,2}^2\boldsymbol{I} \end{bmatrix} \prec \boldsymbol{0}, \quad (17)$$

where $\boldsymbol{N} = \boldsymbol{F}\boldsymbol{S}$.

Due to the lack of space, proofs of *Theorem 1* and *Theorem 2* are not given in an explicit way. After some lengthy but straightforward transformations, they can be obtained using a hybrid mixture of authors' results concerning fault estimation Buciakowski et al. (2017) and FTC Witczak et al. (2016). The main distinction between the results presented in Buciakowski et al. (2017); Witczak et al. (2016) and those proposed in this paper is that the former one do not take into separation between $\boldsymbol{\varepsilon}_k$ and $\boldsymbol{v}_k$, which introduces a significant level of conservatives. They also do not take into account shaping the closed-loop system response, which is undertaken in the subsequent sections.

5. LMI DESIGN PROCEDURE FOR FTC

The problem of determining the observer and controller gain matrices described by *Theorem 1* and *Theorem 2*, respectively, can be treated as an optimization problem aiming at minimizing the disturbance attenuation levels $\mu_{o,1}$, $\mu_{o,2}, \mu_{c,1}$, $\mu_{c,2}$, respectively. This optimization problem can be defined as:

$$\begin{aligned} &\underset{\gamma_{o,1}>0,\gamma_{o,2}>0}{\text{minimize}} && \gamma_{o,1} + \gamma_{o,2} \\ &\text{subject to} && (14), (15), \end{aligned} \quad (18)$$

with a $\gamma_{o,1} = \mu_{o,1}^2$ and $\gamma_{o,2} = \mu_{o,2}^2$ for the observer case while it is

$$\begin{aligned} &\underset{\gamma_{c,1}>0,\gamma_{c,2}>0}{\text{minimize}} && \gamma_{c,1} + \gamma_{c,2} \\ &\text{subject to} && (16), (17). \end{aligned} \quad (19)$$

with $\gamma_{c,1} = \mu_{c,1}^2$ and $\gamma_{c,2} = \mu_{c,2}^2$ for the controller case.

Moreover, the above cost functions (18) and (19) can be transformed into finding a trade off between disturbance attenuation levels $\mu_{o,1}$ and $\mu_{o,2}$ for observer and $\mu_{c,1}$ and $\mu_{c,2}$ for controller by introduction weighting variables $\alpha_o \in (0,1)$ for $\gamma_{o,1}$ and $\gamma_{o,2}$ and $\alpha_c \in (0,1)$, which boils down to:

$$\begin{aligned} \underset{\gamma_{o,1}>0,\gamma_{o,2}>0}{\text{minimize}} \quad & (1-\alpha_o)\gamma_{o,1} + \alpha_o\gamma_{o,2} \\ \text{subject to} \quad & (14), (15). \end{aligned} \tag{20}$$

for the observer case and

$$\begin{aligned} \underset{\gamma_{c,1}>0,\gamma_{c,2}>0}{\text{minimize}} \quad & (1-\alpha_c)\gamma_{c,1} + \alpha_c\gamma_{c,2} \\ \text{subject to} \quad & (16), (17). \end{aligned} \tag{21}$$

for the controller case.

Taking into account the above considerations, a complete integrated FTC design procedure can be summarized as follows:

Off-line computation:

(1) for a predefined α_o solve (20);
(2) calculate $\bar{\boldsymbol{K}} = \boldsymbol{P}^{-1}\boldsymbol{N}$ and $\begin{bmatrix}\boldsymbol{K}\\ \boldsymbol{L}\end{bmatrix} = \bar{\boldsymbol{K}}$;
(3) for a predefined α_c solve (21);
(4) calculate $\boldsymbol{F} = \boldsymbol{N}\boldsymbol{S}^{-1}$;

On-line computation (for each k):

(1) compute the fault estimate $\hat{\boldsymbol{f}}_k$ with (4)–(5);
(2) compute $\boldsymbol{u}_k$ with (8);

6. ILLUSTRATIVE EXAMPLE

This section presents an empirical verification of the proposed approach. For that purpose, a DC servo–motor given in Buciakowski et al. (2017) was considered and the remaining system matrices were as follows:

$$\boldsymbol{A} = \begin{bmatrix} 1.0000 & 0.1000 & 0 \\ 0 & 0.8495 & 0.4977 \\ 0 & -0.0357 & 0.9995 \end{bmatrix}, \quad \boldsymbol{B} = \begin{bmatrix} 0 \\ 0 \\ 0.0729 \end{bmatrix},$$

$$\boldsymbol{C}_o = \begin{bmatrix} 1 & 0 & 0 \\ 0 & 1 & 0 \end{bmatrix}, \quad \boldsymbol{C}_c = [1 \ 0 \ 0],$$

$$\boldsymbol{W}_1 = \begin{bmatrix} 0.5 \\ 0 \\ 0 \end{bmatrix}, \quad \boldsymbol{W}_{o,2} = \begin{bmatrix} 0.05 & 0 \\ 0 & 0.05 \end{bmatrix}, \quad \boldsymbol{W}_{c,2} = 0.05,$$

with $\boldsymbol{x}_k = [\theta, \, v, \, i]^T$ where θ is the angular velocity of the motor, and v is the velocity of the motor and i is the armature current.

Subsequently, the initial conditions for the system and the observer are:

$$\boldsymbol{x}_0 = [0, \, 0, \, 0]^T, \quad \hat{\boldsymbol{x}}_0 = [50, \, 20, \, 10]^T, \quad \hat{\boldsymbol{f}}_0 = \boldsymbol{0}.$$

The reference θ is chosen as $100[rad]$. The signal $\boldsymbol{w}_{1,k}$ was chosen as a step one with the time duration of $20[s]$ and $\boldsymbol{w}_{2,k}$ is chosen as a periodic square signal with time duration $0.2[s]$. Matrices $\boldsymbol{C}_o$ and $\boldsymbol{W}_{o,2}$ are used to calculate observer gain matrices $\boldsymbol{K}$ and $\boldsymbol{L}$, while matrices $\boldsymbol{C}_c$ and $\boldsymbol{W}_{c,2}$ are used to obtain the controller gain matrix $\boldsymbol{F}$.

At the beginning, substituting $\boldsymbol{C} = \boldsymbol{C}_o$, $\boldsymbol{W}_2 = \boldsymbol{W}_{o,2}$ into (6)–(7) and solving the optimization problem (20) for $\alpha_o = 0.001$ give:

$$\bar{\boldsymbol{K}} = \begin{bmatrix}\boldsymbol{K}\\ \boldsymbol{L}\end{bmatrix} = \begin{bmatrix} 0.9930 & 0.1002 \\ 0.0000 & 1.2809 \\ -0.0002 & 0.9919 \\ \hline -0.0021 & 2.1985 \end{bmatrix}, \tag{22}$$

with $\mu_{o,1} = 0.1278$ and $\mu_{o,1} = 6.5767$. Subsequently, for designated parameters, Figs. 2–3 show singular values of the transfer functions $\boldsymbol{G}_{\boldsymbol{e}_f\bar{\boldsymbol{v}}}(z)$ and $\boldsymbol{G}_{\boldsymbol{e}_f\boldsymbol{\varepsilon}}(z)$. Next,

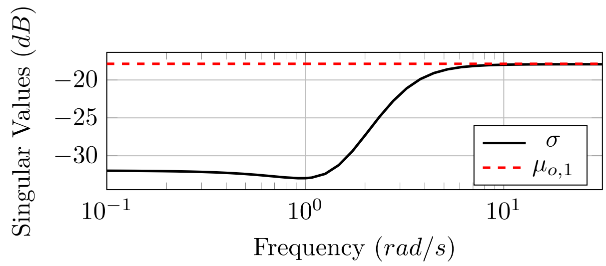

Fig. 2. Singular values of the transfer function $\boldsymbol{G}_{\boldsymbol{e}_f\bar{\boldsymbol{v}}}(z)$

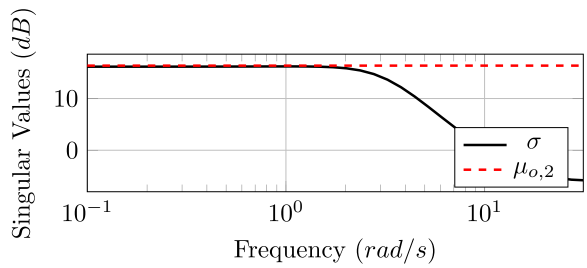

Fig. 3. Singular values of the transfer function $\boldsymbol{G}_{\boldsymbol{e}_f\boldsymbol{\varepsilon}}(z)$

substituting $\boldsymbol{C} = \boldsymbol{C}_c$, $\boldsymbol{W}_2 = \boldsymbol{W}_{c,2}$ in to (9)–(10) and solving optimization problem (21) for $\alpha_c = 0.75$, gives:

$$\boldsymbol{F} = [640.1341 \ 124.5959 \ 50.2044]. \tag{23}$$

with $\mu_{c,1} = 1.1457$ and $\mu_{c,1} = 0.0464$. From the above results, it is evident that the values of the controller gain matrix $\boldsymbol{F}$ have large values, which is not often accepted in practice. To solve this problem a modification of the output matrix $\boldsymbol{C}_c = [1, \, 1, \, 1]$. Note that it is a technical trick as the full state estimate is available.

In all above cases, it is assumed that sum of all energy from $\boldsymbol{v}_k$ and $\boldsymbol{e}_{f,k}$ to output $\boldsymbol{y}_k$ will be minimized. It is important to note that modification of this matrix $\boldsymbol{C}_c$ is needed for solving the optimization problem (21), only. Solving again (21) for $\alpha_c = 0.75$ gives

$$\boldsymbol{F} = [15.0215 \ 13.8383 \ 21.8474], \tag{24}$$

with $\mu_{c,1} = 0.5085$ and $\mu_{c,1} = 0.0942$. The corresponding singular values of the transfer functions $\boldsymbol{G}_{\boldsymbol{y}_f\boldsymbol{v}}(z)$ and $\boldsymbol{G}_{\boldsymbol{y}_f\boldsymbol{e}_f}(z)$ are portrayed in Figs. 4–5. To verify the performance of the close-loop system, the singular values of the sensitivity function S and the complementary sensitivity function T defined as

$$S = 1 - \Phi_1\Phi_2, \quad T = 1 - S, \tag{25}$$

where $\Phi_1 = (\boldsymbol{C}_c(z\boldsymbol{I} - (\boldsymbol{A} - \boldsymbol{B}\boldsymbol{F}))^{-1}\boldsymbol{B})$ and $\Phi_2 = (\boldsymbol{F}(z\boldsymbol{I} - (\boldsymbol{A} - \boldsymbol{K}\boldsymbol{C}_o))^{-1}\boldsymbol{K})$ for portrayed in Figs. 6–7. The results show that for the first channel the function T (dash–dot black line) and S (black solid line) have good shapes, this means that the close loop system for this channel has a good disturbance and noise rejection characteristics as well

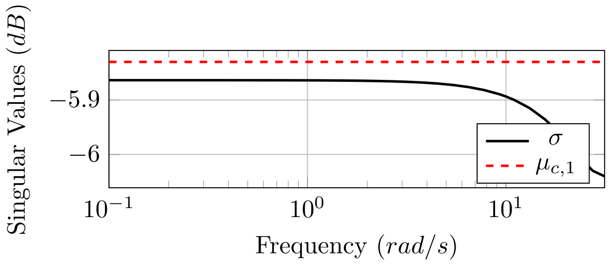

Fig. 4. Singular values of the transfer function $\boldsymbol{G}_{\boldsymbol{y}_f\boldsymbol{v}}(z)$

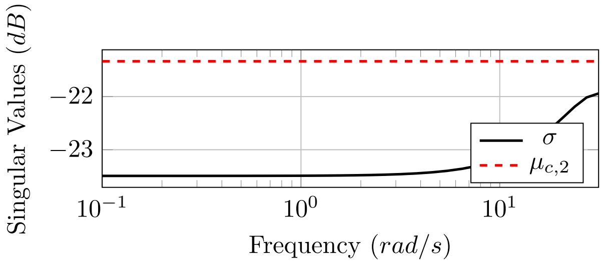

Fig. 5. Singular values of the transfer function $\boldsymbol{G}_{\boldsymbol{y}_f\boldsymbol{e}_f}(z)$

as good tracking performance. On the other hand, for the second channel function T (dash–dot black line) and S (black solid line) are not as good as the characteristics for the first one. In order to solve this problem and improve the characteristics of T and S, it is proposed to use shaping filter W for changing the shape of function S. To handle this issue, the following algorithm for designing the controller gain matrix $\boldsymbol{F}$ is proposed:

Step 1: Design observer gain matrices $\boldsymbol{K}$ and $\boldsymbol{L}$ using optimization problem (20).
Step 2: Solve optimization problem (21) to get an initial value of controller gain matrix $\boldsymbol{F}$.
Step 3: Select shaping filter W for function S.
Step 4: Select scaling factor ζ to decrease or increase the gain of matrix $\boldsymbol{F}$.
Step 5: Solve the following optimization problem

$$\underset{\zeta \boldsymbol{F}}{\text{minimize}} \quad \|WS\|_\infty < 1. \tag{26}$$

Using the above algorithm and arbitrarily selecting shaping filter

$$W = \frac{0.9z - 0.8}{z - 0.9999}, \tag{27}$$

after 100 iterations the results are:

$$\|WS\|_\infty = 1.7660, \quad \boldsymbol{F} = [4.4811 \; 2.6277 \; 7.4235], \tag{28}$$

and hence controller gains are no longer unacceptably large. Figs. 6–7 show singular values of the sensitivity function S (solid red line) and complementary sensitivity function T (dash–dot black line) as well as singular values of shaping filter W (dotted blue line) after solving optimization problem (26). The results show that close loop system for each channel has good disturbance and noise rejection characteristics as well as good tracking performance. Finally, in order to verify in time domain performance of proposed approach related to fault compensation and disturbance rejection the following Simulation Case (SCs) are proposed:

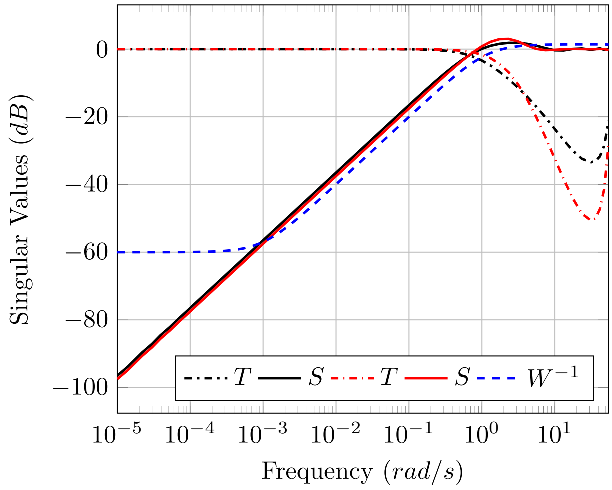

Fig. 6. Singular values from input 1 to output with shaping filter: S (solid red line), T (dash dot red line) and without shaping filter: S (black solid line), T (dash dot black line) and shaping filter W^{-1} (dotted blue line)

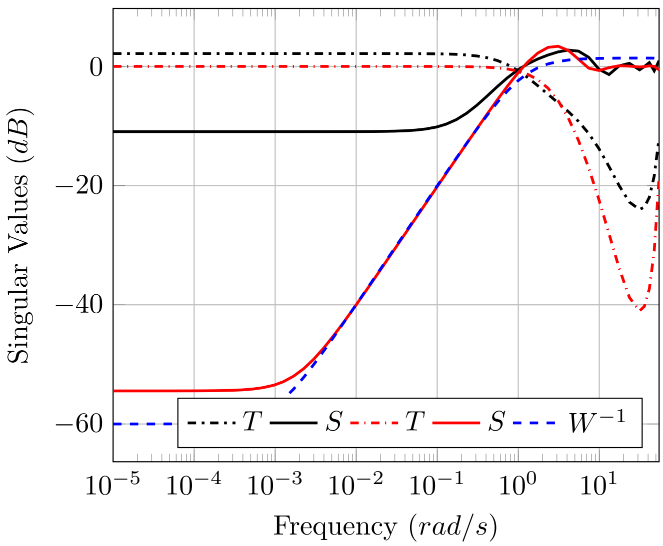

Fig. 7. Singular values from input 2 to output with shaping filter: S (solid red line), T (dash dot red line) and without shaping filter: S (black solid line), T (dash dot black line) and shaping filter W^{-1} (dotted blue line)

SC1: Observer parameters given by (22) and controller parameters in the form (24);
SC2: Observer parameters given by (22) and controller parameters in the form (28).

For each simulation case, the following fault scenario (FS) treated as a 10% decrease in actuator performance is proposed:

$$\boldsymbol{f}_k = \begin{cases} -0.10 & 40 \le t \le 50, \\ 0 & \text{otherwise.} \end{cases}$$

Figs. 8–9 present the system state variable θ for SC1, SC2 and FS with and without FTC strategy. The control strategy without FTC (i.e., $\boldsymbol{u}_k = -\boldsymbol{F}\boldsymbol{x}_k$), which is a robust control only, does not consider any information about faults. Thus, it is impossible to be realize suitable recovery actions (Fig. 8). Contrarily, the control strategy with FTC (i.e. $\boldsymbol{u}_k = -\boldsymbol{F}\boldsymbol{x}_k - \hat{\boldsymbol{f}}_k$) gives significantly better performance, which is exhibited in Fig. 9. Moreover, Figs. 8–9 show the system response for disturbance $\boldsymbol{w}_{1,k}$. It can be seen that for SC1 the amplitude of the state variable θ is greater than the amplitude for SC2. This is due to the fact that close loop system for controller designed using the proposed algorithm with shaping S function provides better disturbance and noise rejection characteristics than SC1. Additionally, from Figs. 8–9 it can be deduced that response to the actuator fault for SC2 has a lower amplitude than SC1. This is a very important feature form practical viewpoint.

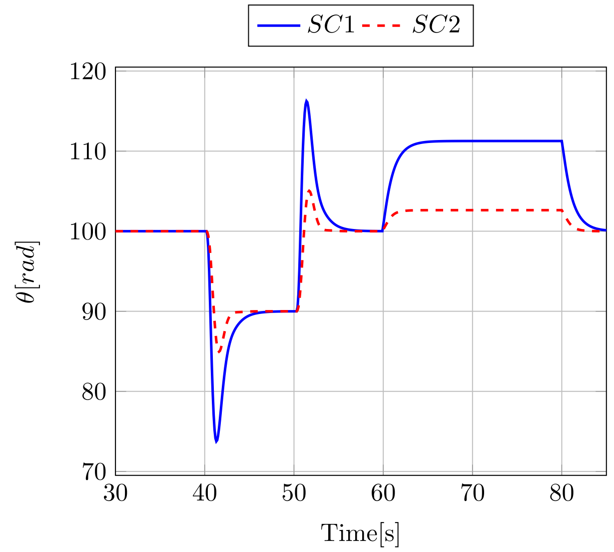

Fig. 8. State variable θ for SC1 (blue solid line), SC2 (red doted line) and response for fault signal at time $40 \leq t \leq 50$ and response for disturbance signal $\boldsymbol{w}_{1,k}$ at time $60 \leq t \leq 80$ without FTC (i.e. $\boldsymbol{u}_k = -\boldsymbol{F}\boldsymbol{x}_k$)

7. CONCLUSIONS

The main objective of the paper was to proposed a novel design procedure of an integrated FTC. It avoids three-step fault diagnosis procedure and replaces by the fault estimation. The inaccuracies caused by fault estimation are taken into account while designing fault-tolerant controller. However, they do not simply extend the set of disturbances/noise. They are taken into account individually in such a way as to achieve a well-balanced final control effect. This results in the FTC design procedure that can be tailored to various system behaviors, which may arise in control engineering practice. The performance of the proposed approach is illustrated with a DC servo–motor benchmark example. The obtained results clearly exhibits benefits related to its application.

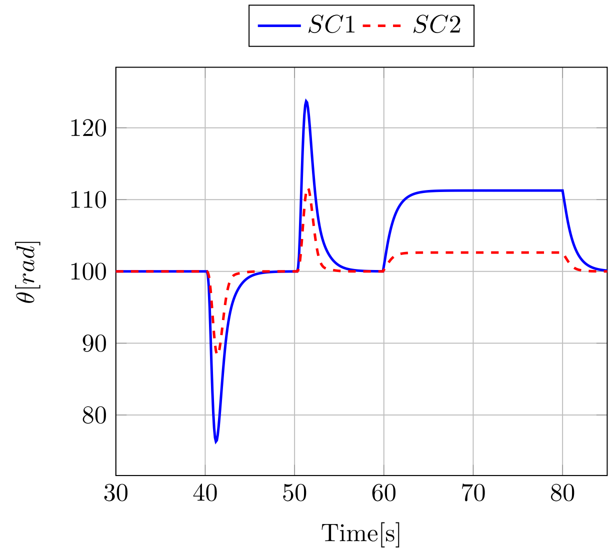

Fig. 9. State variable θ for SC1 (blue solid line), SC2 (red doted line) and response for fault signal at time $40 \leq t \leq 50$ and response for disturbance signal $\boldsymbol{w}_{1,k}$ at time $60 \leq t \leq 80$ with FTC (i.e. $\boldsymbol{u}_k = -\boldsymbol{F}\boldsymbol{x}_k - \hat{\boldsymbol{f}}_k$)

REFERENCES

Blanke, M., Kinnaert, M., Lunze, J., and Staroswiecki, M. (2006). *Diagnosis and Fault-Tolerant Control*. Second Edition. Springer-Verlag Berlin Heidelberg.

Buciakowski, M., Witczak, M., Mrugalski, M., and Theilliol, D. (2017). A quadratic boundedness approach to robust dc motor fault estimation. *Control Engineering Practice*, 66, 181 – 194.

Chen, J. and Patton, R.J. (1999). *Robust Model-based Fault Diagnosis for Dynamic Systems*. Kluwer Academic Publishers, London.

Ding, S. (2008). *Model-based Fault Diagnosis Techniques: Design Schemes, Algorithms, and Tools*. Springer-Verlag, Berlin, Heidelberg.

Isermann, R. (2006). *Fault Diagnosis Systems. An Introduction from Fault Detection to Fault Tolerance*. Springer-Verlag, New York.

Mejdi, S., Messaoud, A., and Abdennour, R.B. (2020). Fault tolerant multicontrollers for nonlinear systems: A real validation on a chemical process. *Int. J. Appl. Math. Comput. Sci*, 30(1), 61–74.

Pazera, M., Buciakowski, M., and Witczak, M. (2018). Robust multiple sensor fault–tolerant control for dynamic non–linear systems: Application to the aerodynamical twin–rotor system. *Int. J. Appl. Math. Comput. Sci*, 28(2), 297–308.

Salazar, J.C., Sanjuan, A., Nejjari, F., and Sarrate, R. (2020). Health–aware and fault-tolerant control of an octorotor uav system based on actuator reliability. *Int. J. Appl. Math. Comput. Sci*, 30(1), 47–59.

Witczak, M., Buciakowski, M., and Aubrun, C. (2016). Predictive actuator fault-tolerant control under ellipsoidal bounding. *International Journal of Adaptive Control and Signal Processing*, 30(2), 375–392.

Witczak, M., Buciakowski, M., and Mrugalski, M. (2014). An $\mathcal{H}_\infty$ approach to fault estimation of non-linear systems: Application to one-link manipulator. In *19th International Conference On Methods and Models in Automation and Robotics (MMAR) 2014*, 456–461. IEEE.

Zhang, Y. and Jiang, J. (2008). Bibliographical review on reconfigurable fault-tolerant control systems. *Annual Reviews in Control*, 32(2), 229–252.